Applications of Mathematics

Yoshiki Sugitani

Numerical analysis of a Stokes interface problem based on formulation using the characteristic function

Applications of Mathematics, Vol. 62 (2017), No. 5, 459–476

Persistent URL: http://dml.cz/dmlcz/146916

NUMERICAL ANALYSIS OF A STOKES INTERFACE PROBLEM BASED ON FORMULATION USING THE CHARACTERISTIC FUNCTION

Yoshiki Sugitani, Sendai

Received December 28, 2016. First published October 9, 2017.

Abstract. Numerical analysis of a model Stokes interface problem with the homogeneous Dirichlet boundary condition is considered. The interface condition is interpreted as an additional singular force field to the Stokes equations using the characteristic function. The finite element method is applied after introducing a regularization of the singular source term. Consequently, the error is divided into the regularization and discretization parts which are studied separately. As a result, error estimates of order $h^{1/2}$ in $H^1 \times L^2$ norm for the velocity and pressure, and of order h in L^2 norm for the velocity are derived. Those theoretical results are also verified by numerical examples.

Keywords: interface problem; Stokes equation; finite element method

MSC 2010: 65N30, 65N15, 74F10, 74A50, 76D07

1. Introduction

In the study of multi-phase flow problems of viscous incompressible fluids, we often encounter the Navier-Stokes equations with an interface condition

$$\frac{\partial u}{\partial t} + (u \cdot \nabla)u - \nu \Delta u + \frac{1}{\varrho}\nabla p = h(x,t), \quad \nabla \cdot u = 0 \quad \text{in } \Omega \times (0,T), \tag{1a}$$

$$u = 0 \quad \text{on } \partial\Omega \times (0,T), \tag{1b}$$

$$[u] = 0, \quad [\tau] = g(x,t) \quad \text{on } \Gamma \times (0,T), \tag{1c}$$

$$u(x,0) = u^{(0)}(x) \quad \text{in } \Omega, \tag{1d}$$

where u and p denote the velocity and pressure, respectively, and $T < \infty$. Herein, Ω denotes a fixed bounded domain in $\mathbb{R}^d$, $d = 2, 3$, with the boundary $\partial\Omega$, and Γ is

This work was supported by JST CREST Grant Number JPMJCR15D1, Japan.

a closed surface/curve included in Ω which represents the interface. The coefficient of kinetic viscosity ν is assumed to be a piecewise constant function ($\nu = \nu_1$ inside Γ and $\nu = \nu_2$ outside Γ for example). The traction (or stress) vector is denoted by τ (see Section 2 for the precise definition). Moreover, $[\cdot]$ stands for the jump across the interface Γ. Here $h(x,t), g(x,t)$, and $u^{(0)}(x)$ are given functions. There is numerous literature devoted to numerical methods for these kinds of interface problems (see [5], [9], [18] for example). In particular, the variational formulation of (1) is directly discretized by the finite element method (see [2] and [19]). However, it is non-trivial to implement the boundary integral term $\int_\Gamma g(x,t)v(x)\,\mathrm{d}x$ for the finite difference and finite volume methods. Even if we use the finite element method, the approximation of the boundary integral term is quite technical. In order to avoid those difficulties, the *immersed boundary (IB) method* is frequently applied, which was proposed by Peskin [15] originally for solving a class of fluid-structure interaction problems [13], [14]. In the IB method, the interface problem (1) is equivalently reformulated to partial differential equations stated below. Let $\Gamma(t)$ be parameterized as $\Gamma(t) = \{X(\theta,t) = (X_1(\theta,t),\dots,X_d(\theta,t));\ \theta \in \Theta\}$ for the Lagrangian coordinate $\theta \in \mathbb{R}^{d-1}$. Here $\Theta \subset \mathbb{R}^{d-1}$ is the set of all θ and denotes the reference configuration. Then the interface condition (1c) is interpreted as an outer force field f defined on Ω and included in the Navier-Stokes equations such that

$$\text{(2a)} \qquad \frac{\partial u}{\partial t} + (u\cdot\nabla)u - \nu\Delta u + \nabla p = h + f, \quad \nabla\cdot u = 0 \quad \text{in } \Omega\times(0,T),$$

$$\text{(2b)} \qquad u = 0 \quad \text{on } \partial\Omega\times(0,T),$$

$$\text{(2c)} \qquad u(x,0) = u^{(0)}(x) \quad \text{in } \Omega,$$

$$\text{(2d)} \qquad f(x,t) = \int_\Theta F(\theta,t)\delta(x - X(\theta,t))\,\mathrm{d}\theta.$$

Herein, F denotes the force density distributed along $\Gamma(t)$, and δ is the Dirac delta function. For computation, we solve (2) together with the equation of the interface motion $\partial X/\partial t = u(X,t)$. The problem (2) was first introduced to investigate blood flow in the presence of cardiac valves, in which $\Gamma(t)$ corresponded to the position of heart valves regarded as a thin elastic structure, and $F(\theta,t)$ represented the effect of them. The main advantage of this method is that we can use fixed uniform meshes. Consequently, the equation can be discretized not only by the finite element method but also by the finite difference method. Moreover, $f(x,t)$ is replaced by a regularized outer force $f^\varepsilon(x,t)$ using a smooth approximation to Dirac delta function. Then the value of $f^\varepsilon(x,t)$ is calculated by simple quadrature formulas. The IB method is recognized to be one of most powerful methods for the interface problems of fluid-structure interaction and it is widely applied at present. However, there are only a few results about the theoretical convergence analysis in contrast to a huge number

of applications. In a previous paper, Saito and Sugitani [17], we have studied the convergence of the IB method for a model stationary Stokes problem, where the immersed force field is approximated using a regularized delta function and the error in the $W^{-1,p}$ norm is examined for $1 \leqslant p \leqslant d/(d-1)$. Then we consider the immersed boundary discretization of the Stokes problem and study the regularization and discretization errors separately. Consequently, error estimate of order $h^{1-\alpha}$ in the $W^{1,1} \times L^1$ norm for the velocity and pressure is derived, where α is an arbitrarily small positive number. Error estimate of order $h^{1-\alpha}$ in the L^r norm for the velocity is also derived with $r = d/(d-1-\alpha)$. However, optimal order and L^2 error estimates are still open at present.

At this stage, it is worth recalling that a simpler reformulation method for (1) was proposed by Fujita et al. [6] in 1995. Their reformulation reads as

$$\text{(3a)} \quad \frac{\partial u}{\partial t} + (u \cdot \nabla)u - \nu \Delta u + \nabla p = h + \tilde{g}(\nabla \chi \cdot \tilde{n}), \quad \nabla \cdot u = 0 \quad \text{in } \Omega \times (0,T),$$

$$\text{(3b)} \quad u = 0 \quad \text{on } \partial\Omega \times (0,T),$$

$$\text{(3c)} \quad u(x,0) = u^{(0)}(x) \quad \text{in } \Omega.$$

Herein, χ denotes the characteristic function of the region surrounded by $\Gamma(t)$ in Ω, and n is the unit normal vector to $\Gamma(t)$. Functions $\tilde{g}$ and $\tilde{n}$ stand for the smooth extensions of g and n into Ω, respectively. The reformulation (3) is discretized by the finite element and finite difference methods using fixed uniform meshes as well as the IB reformulation. Formulation (3) is essentially equivalent to the IB formulation (2), whereas (3) seems to be easier to deal with both mathematically and practically since there are no Lagrangian coordinates and no need to generate moving fine mesh along $\Gamma(t)$ for each time step. In [6], the derivation of the reformulation and some numerical results are presented. However, no mathematical analysis including convergence is given.

Our ultimate objective is to study the convergence of the above reformulation using the characteristic function. In this paper, as a first step, we deal with a model interface problem for the stationary Stokes equations with fixed interface Γ (supposed to be a thin elastic body) since the Stokes problem naturally arises when solving FSI problems for Navier-Stokes equations using the weak coupling approach. Then, following [17], we study the regularization and discretization errors separately. We state our model problem in the classical form and its *weak formulation* in Section 2. Then, since the derivative of the characteristic function $\nabla\chi$ has singularities on Γ, regularization is required. We state our regularization procedure and examine its error in Section 3. As a matter of fact, the $H^1 \times L^2$ error between regularized and original problems is estimated to be of order $\varepsilon^{1/2}$ (see Proposition 3.2). Section 4 is devoted to the finite element approximation by MINI (P1b/P1) finite element.

Theorem 4.1, the main result of this paper, offers error estimates for the discretization parameter $h > 0$. That is, the $H^1 \times L^2$ error for velocity and pressure converges at order $h^{1/2}$, while the L^2 error for velocity has a first order convergence. Finally, we confirm our results by numerical experiments in Section 5. We verify that desired convergence rates are obtained with uniform mesh.

2. Stokes interface problem

2.1. Geometry and notation. Let Ω be a polyhedral domain in $\mathbb{R}^d (d = 2, 3)$ with boundary $\partial\Omega$. We suppose that Ω is divided into two disjoint subdomains Ω_0 and Ω_1 by a simple Lipschitz curve ($d = 2$) or surface ($d = 3$) denoted by Γ. We assume that the interface Γ is closed ($\partial\Omega \cap \bar{\Gamma} = \emptyset$), or goes across Ω ($\partial\Omega \cap \bar{\Gamma} \neq \emptyset$). For example, see Figure 1. In both cases, the boundaries $\partial\Omega_i (i = 0, 1)$ are Lipschitz boundaries.

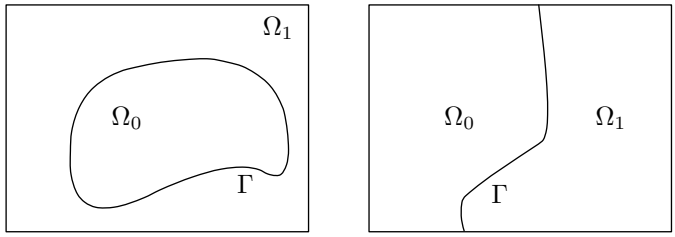

Figure 1. Example of Ω with $\partial\Omega \cap \bar{\Gamma} = \emptyset$ (left) and $\partial\Omega \cap \bar{\Gamma} \neq \emptyset$ (right).

For function spaces and their norms, we follow the notation of [1]. The standard Lebesgue and Sobolev spaces such as $L^2(\Omega), H^1(\Omega), W^{1,\infty}(\Omega)$, $L^2(\Gamma)$, and $W^{2-1/p,p}(\Gamma)$ with some $p > d$ will be used. We set $H^1_0(\Omega) = \{v \in H^1(\Omega);\ v|_{\partial\Omega} = 0\}$ and $L^2_0(\Omega) = \{q \in L^2(\Omega);\ \int_\Omega q \,\mathrm{d}x = 0\}$. For a function space X, the symbol X^d denotes the product space $X \times \ldots \times X$. The norm notation is abbreviated by

$$\|u\|_{H^1} = \|u\|_{H^1(\Omega)^d}, \quad \|p\|_{L^2} = \|p\|_{L^2(\Omega)}. \tag{4}$$

The symbol H^{-1} stands for the dual space of $H^1_0(\Omega)$ and the dual product between $H^{-1}(\Omega)^d$ and $H^1_0(\Omega)^d$ is written as $\langle \cdot, \cdot \rangle = \langle \cdot, \cdot \rangle_{H^{-1}, H^1_0}$. Moreover, the inner product of $L^2(\Omega)^d$ is denoted by $(\cdot, \cdot)_{L^2}$.

2.2. Model Stokes interface problem and equivalent formulations. We consider the following model Stokes interface problem:

$$-\nu\Delta u_i + \nabla p_i = 0, \quad \nabla \cdot u_i = 0 \quad \text{in } \Omega_i, \tag{5a}$$

$$u_i = 0 \quad \text{on } \partial\Omega_i \setminus \Gamma, \quad i = 0, 1, \tag{5b}$$

$$u_0 = u_1, \quad \tau_0 + \tau_1 = g \quad \text{on } \Gamma, \tag{5c}$$

for velocity u_i and pressure p_i with density $\varrho = 1$ and kinetic viscosity $\nu_0 = \nu_1 = \nu > 0$, respectively, in Ω_i, $i = 0, 1$. Here τ_i denotes the traction vector defined by

$$\tau_i = \sigma(u_i, p_i)n_i, \tag{6}$$

where $\sigma(u,p) = (\sigma_{jk}(u,p))_{1\leqslant j,k\leqslant d} = -pI + \nu(\nabla u + \nabla u^{\mathrm{T}})$ is called the stress tensor, I the identity matrix, and n_i the outward unit normal vector to $\partial\Omega_i$. Moreover, g is a prescribed function standing for a jump of tractions across Γ. We assume $g \in L^2(\Gamma)^d$ for the time being.

R e m a r k 2.1. In the model equations (5), we assume $\nu_0 = \nu_1$ in order to avoid the difficulties related to different kinetic viscosities, and focus on the analysis of the reformulation using the characteristic function. In the case of $\nu_0 \neq \nu_1$, the convergence of the finite element solutions is studied by Ohmori and Saito [12] under a suitable geometrical condition on the triangulation.

To deal with the problem precisely, we introduce the notion of *weak solution*. By a *weak solution* to (5), we mean a solution of the following variational equations: Find $(u,p) \in H_0^1(\Omega)^d \times L_0^2(\Omega)$ such that

$$a(u,v) + b(p,v) = \int_\Gamma g \cdot v \,\mathrm{d}\Gamma \quad \forall\, v \in H_0^1(\Omega)^d, \tag{7a}$$

$$b(q,u) = 0 \quad \forall\, q \in L_0^2(\Omega), \tag{7b}$$

where

$$a(u,v) = \frac{\nu}{2}\int_\Omega \Big(\frac{\partial u_j}{\partial x_i} + \frac{\partial u_i}{\partial x_j}\Big)\Big(\frac{\partial v_j}{\partial x_i} + \frac{\partial v_i}{\partial x_j}\Big)\,\mathrm{d}x, \tag{8a}$$

$$b(p,u) = -\int_\Omega p(\nabla \cdot u)\,\mathrm{d}x. \tag{8b}$$

Indeed, if there exists a smooth solution (u_i, p_i) to (5), then (u,p) satisfies (7) with

$$u = \begin{cases} u_0 & \text{in } \Omega_0, \\ u_1 & \text{in } \Omega_1 \end{cases} \qquad \text{and} \qquad p = \begin{cases} p_0 & \text{in } \Omega_0, \\ p_1 & \text{in } \Omega_1. \end{cases} \tag{9}$$

Now we shall verify this. It is obvious that (u,p) defined by (9) belongs to $H_0^1(\Omega)^d \times L^2(\Omega)$, since u is continuous on Γ and vanishes on $\partial\Omega$. Further, since $\nabla \cdot u_i = 0$ in Ω_i, u satisfies (7b). In order to derive (7a), multiply (5a) by $v \in C_0^\infty(\Omega)^d$ and integrate over Ω_i. Then we have

$$-\nu\int_{\Omega_i} \Delta u_i \cdot v|_{\Omega_i}\,\mathrm{d}x + \int_{\Omega_i} \nabla p_i \cdot v|_{\Omega_i}\,\mathrm{d}x = 0 \quad \forall\, v \in C_0^\infty(\Omega)^d,\ i = 0, 1. \tag{10}$$

Using the density of $C_0^\infty(\Omega)^d$ in $H_0^1(\Omega)^d$, Green's formula, and summing up the two equations, we obtain

$$a(u,v) + b(p,v) = \int_\Gamma (\sigma(u_0,p_0)n_0 + \sigma(u_1,p_1)n_1)\cdot v \,\mathrm{d}\Gamma \quad \forall\, v \in H_0^1(\Omega)^d. \tag{11}$$

Because of the jump condition (5c), the right-hand side equals $\int_\Gamma g \cdot v \,\mathrm{d}\Gamma$. This discussion remains true if p_i is replaced by $p_i + c$ with any $c \in \mathbb{R}$. Finally, we can choose $c \in \mathbb{R}$ such that $\int_\Omega (p+c)\,\mathrm{d}x = 0$.

Since $v \mapsto \int_\Gamma g \cdot v \,\mathrm{d}\Gamma$ for $g \in L^2(\Gamma)^d$ is a bounded linear functional on $H_0^1(\Omega)^d$, the well-posedness of (7) is proved by the standard theory. We recall the following result.

Lemma 2.1 (cf. [10] and [4]). *Let Ω be a connected, bounded, convex polyhedral domain of $\mathbb{R}^d$, and let h be in $H^{-1}(\Omega)^d$. Then there exists a unique weak solution $(w,r) \in H_0^1(\Omega)^d \times L_0^2(\Omega)$ of the Stokes problem*

$$-\nu\Delta w + \nabla r = h \text{ in } \Omega, \quad \nabla\cdot w = 0 \quad \text{in } \Omega, \quad w = 0 \quad \text{on } \partial\Omega \tag{12}$$

satisfying

$$\|w\|_{H^1} + \|r\|_{L^2} \leqslant C_1 \|h\|_{H^{-1}}. \tag{13}$$

Moreover, if $h \in L^2(\Omega)^d$, we have $(w,r) \in H^2(\Omega)^d \times H^1(\Omega)$ and

$$\|w\|_{H^2} + \|r\|_{H^1} \leqslant C_2 \|h\|_{L^2}. \tag{14}$$

Herein, C_1 and C_2 denote positive constants depending only on Ω.

Now we proceed to derive an equivalent formulation to (7). To this end, we assume
(A1) Γ is of class C^2,
(A2) $g \in W^{2-1/p,p}(\Gamma)^d$ with some $p > d$.
According to [6], (1.17), we have

$$\int_\Gamma g\cdot\varphi \,\mathrm{d}\Gamma = \langle \tilde{g}(\nabla\chi\cdot\tilde{n}), \varphi\rangle \quad \forall\, \varphi \in C_0^\infty(\Omega)^d, \tag{15}$$

where χ is the characteristic function of Ω_0 in Ω, i.e.,

$$\chi(x) = \begin{cases} 1 & x \in \Omega_0, \\ 0 & x \notin \Omega_0. \end{cases} \tag{16}$$

Moreover, $\tilde{n}$ is a C^1 extension of n_1 into Ω and $\tilde{g}$ is the extension of g given by the following lemma. For the reader's convenience, we recall the proof of (15) in Appendix A.

Lemma 2.2. *Suppose that* (A1) *and* (A2) *are satisfied. Then there exists a* $\tilde{g} \in W^{2,p}(\Omega)^d \cap W^{1,\infty}(\Omega)^d$ *such that* $\tilde{g} = g$ *on* Γ *and*

$$\|\tilde{g}\|_{W^{1,\infty}(\Omega)^d} \leqslant C_0 \|g\|_{W^{2-1/p,p}(\Gamma)^d}, \tag{17}$$

where C_0 *denotes a positive constant depending only on* Γ *and* Ω.

The proof is a consequence of the lifting-extension theorem (see [11], Theorem 2-5.8 and Theorem 2-3.9), and the Sobolev embedding theorem (cf. [1], Theorem 4.12).

At this stage, we set

$$f = \tilde{g}(\nabla\chi \cdot \tilde{n}). \tag{18}$$

Then we still have $f \in H^{-1}(\Omega)^d$ and state an equivalent formulation to (7): Find $(u, p) \in H_0^1(\Omega)^d \times L_0^2(\Omega)$ such that

$$a(u, v) + b(p, v) = \langle f, v\rangle_{H^{-1}, H_0^1} \quad \forall\, v \in H_0^1(\Omega)^d, \tag{19a}$$

$$b(q, u) = 0 \quad \forall\, q \in L_0^2(\Omega). \tag{19b}$$

Finally, writing down the strong form of (19), we obtain the Stokes equations with the singular source term defined by (18):

$$-\nu\Delta u + \nabla p = f \text{ in } \Omega, \quad \nabla \cdot u = 0 \text{ in } \Omega, \quad u = 0 \text{ on } \partial\Omega. \tag{20}$$

which is equivalent to our problem (5) in the distribution sense.

R e m a r k 2.2. Problem (7) can be directly discretized by the finite element method using the boundary integral on Γ. Such methods were studied in [2] and [19] for nonstationary Navier-Stokes equations. However, in order to avoid the *moving mesh problem*, we study the formulation (19) and apply the finite element method to it using a uniform mesh.

3. Regularization to the distribution form with characteristic function

As explained in Introduction, for computation using a uniform mesh, we introduce a regularized force field $f^\varepsilon \in L^2(\Omega)^d$ as

$$f^\varepsilon = \tilde{g}(\nabla \chi^\varepsilon \cdot \tilde{n}). \tag{21}$$

Herein, $\varepsilon > 0$ is a regularization parameter and χ^ε is an appropriate approximation to the characteristic function χ. We assume that χ^ε is a Lipschitz function. For f^ε given as (21), let us consider

$$-\nu\Delta u^\varepsilon + \nabla p^\varepsilon = f^\varepsilon \ \text{ in } \Omega, \quad \nabla \cdot u^\varepsilon = 0 \ \text{ in } \Omega, \quad u^\varepsilon = 0 \ \text{ on } \partial\Omega. \tag{22}$$

Since $f^\varepsilon \in L^2$, there exists a unique weak solution $(u^\varepsilon, p^\varepsilon) \in H_0^1(\Omega)^d \times L_0^2(\Omega)$ for all $\varepsilon > 0$. Then, the error of regularization is estimated using Lemma 2.1.

Proposition 3.1. *Let (u, p) and $(u^\varepsilon, p^\varepsilon)$ be the weak solutions of* (20) *and* (22)*, respectively. Then we have*

$$\|u - u^\varepsilon\|_{H^1} + \|p - p^\varepsilon\|_{L^2} \leqslant C^* \|\chi - \chi^\varepsilon\|_{L^2}, \tag{23}$$

where $C^* > 0$ is a positive constant depending only on Ω, Γ, and $\|g\|_{W^{2-1/p,p}}$.

Proof. By virtue of Lemma 2.1, we have

$$\|u - u^\varepsilon\|_{H^1} + \|p - p^\varepsilon\|_{L^2} \leqslant C_1 \|f - f^\varepsilon\|_{H^{-1}}.$$

It remains to bound $\|f - f^\varepsilon\|_{H^{-1}}$ by $\|\chi - \chi^\varepsilon\|_{L^2}$. Indeed, we obtain for all $v \in H_0^1(\Omega)^d$

$$\begin{aligned}
\langle f - f^\varepsilon, v\rangle_{H^{-1}, H_0^1} &= \langle \tilde{g}\nabla(\chi - \chi^\varepsilon) \cdot \tilde{n}, v\rangle_{H^{-1}, H_0^1} \\
&= -(\chi - \chi^\varepsilon, \nabla \cdot (\tilde{n}(\tilde{g} \cdot v)))_{L^2} \\
&\leqslant \|\chi - \chi^\varepsilon\|_{L^2} \|\tilde{n}(\tilde{g} \cdot v))\|_{H^1} \\
&\leqslant \|\tilde{n}\|_{W^{1,\infty}} \|\tilde{g}\|_{W^{1,\infty}} \|\chi - \chi^\varepsilon\|_{L^2} \|v\|_{H^1}.
\end{aligned}$$

Hence, the desired result holds with $C^* = C_0 C_1 \|\tilde{n}\|_{W^{1,\infty}} \|g\|_{W^{2-1/p,p}}$. □

3.1. Construction of χ^ε. Now we define χ^ε as follows:

$$\chi^\varepsilon(x) = \begin{cases} 1, & x \in \Omega_0, \\ \max\Big\{0, 1 - \dfrac{\operatorname{dist}(x, \Gamma)}{\varepsilon}\Big\}, & x \notin \Omega_0. \end{cases} \tag{24}$$

We have $\chi^\varepsilon \in W^{1,\infty}(\Omega)$ and

$$\|\chi - \chi^\varepsilon\|_{L^2(\Omega)} \leqslant C_3\sqrt{\varepsilon}, \tag{25}$$

where C_3 is a positive constant depending only on Γ. To verify this, we set $\Gamma^\varepsilon = \{x \in \Omega_1\,;\ \operatorname{dist}(x,\Gamma) \leqslant \varepsilon\}$ and calculate as (noting that $\chi - \chi^\varepsilon$ equals χ^ε in Γ^ε and vanishes outside)

$$\|\chi - \chi^\varepsilon\|_{L^2(\Omega)} = \|\chi^\varepsilon\|_{L^2(\Gamma^\varepsilon)} \leqslant \underbrace{\|\chi^\varepsilon\|_{L^\infty}}_{\leqslant 1} \operatorname{meas}(\Gamma^\varepsilon)^{1/2} \leqslant C_3\sqrt{\varepsilon}.$$

Therefore, we obtain the regularization error estimate as follows.

Proposition 3.2. *Let (u,p) and $(u^\varepsilon,p^\varepsilon)$ be, respectively, the weak solutions to* (20) *and* (22) *with* (24). *Then we have*

$$\|u - u^\varepsilon\|_{H^1} + \|p - p^\varepsilon\|_{L^2} \leqslant C\sqrt{\varepsilon}. \tag{26}$$

R e m a r k 3.1. Other choices of χ^ε are of course used for implementation. As seen above, it is enough to suppose $\chi^\varepsilon \in W^{1,\infty}$ for error estimates, and the order of regularization error is independent of χ^ε if $\operatorname{supp}|\nabla\chi^\varepsilon| \subset \Gamma^\varepsilon$. Moreover, we can also use the function

$$\chi^\varepsilon(x) = \frac{1}{2}\Big[1 - \frac{2}{\pi}\arctan\Big(\frac{\operatorname{dist}(x,\Gamma)}{\varepsilon}\Big)\Big]. \tag{27}$$

Then we have $\operatorname{supp}\chi^\varepsilon \not\subseteq \Gamma^\varepsilon$, while we can derive the same convergence rates as for (24) by simple calculation.

4. Discretization by finite element method

This section is dedicated to a study of the finite element approximation to (22). Let $\{\mathcal{T}_h\}_h$ be a family of *regular* triangulations of Ω, i.e., there exists $\kappa > 0$ satisfying $h_T \leqslant \kappa\varrho_T$ for all $T \in \mathcal{T}_h$. Here, h_T denotes the diameter of T, ϱ_T the diameter of the inscribed ball of T, and $h = \max\{h_K\,;\ K \in \mathcal{T}_h\}$.

We employ the P1b/P1 (MINI) element for discretization and set

$$V_h = \{v_h \in C(\overline{\Omega})^d \cap H_0^1(\Omega)^d\,;\ v_h|_T \in [\mathcal{P}_1(T) \oplus \mathcal{B}(T)\}]^d\ \forall\, T \in \mathcal{T}_h\},$$
$$Q_h = \{q_h \in C(\overline{\Omega}) \cap L_0^2(\Omega)\,;\ q_h|_T \in \mathcal{P}_1(T)\ \forall\, T \in \mathcal{T}_h\}.$$

Therein, $\mathcal{P}_k(T)$ is the set of all polynomials defined on $T \in \mathcal{T}_h$ of degree $\leqslant k$, and $\mathcal{B}(T) = \operatorname{span}\{\lambda_1\lambda_2 \dots \lambda_{d+1}\}$ is the so-called *bubble* function with λ_i the barycentric coordinates of T. It is well-known that the pair of V_h and Q_h satisfies the uniform Babuška-Brezzi (inf-sup) condition

$$\sup_{v_h \in V_h} \frac{b(v_h, q_h)}{\|v_h\|_{H^1}} \geqslant \kappa_2 \|q_h\|_{L^2}, \quad q_h \in Q_h,$$

where $\kappa_2 > 0$ is independent of h.

R e m a r k 4.1. We deal with the P1b/P1 element only for the sake of simple presentation. Similar results can be obtained for an arbitrary pair of conforming finite element spaces $V_h \subset H^1(\Omega)^d$ and $Q_h \subset L^2_0(\Omega)$ satisfying the uniform Babuška-Brezzi condition.

The finite element approximation to (22) is given as follows: Find $(u_h^\varepsilon, p_h^\varepsilon) \in V_h \times Q_h$ such that

$$a(u_h^\varepsilon, v_h) + b(p_h^\varepsilon, v) = (f^\varepsilon, v_h)_{L^2} \quad \forall\, v_h \in V_h, \tag{28a}$$

$$b(q_h, u_h^\varepsilon) = 0 \quad \forall\, q_h \in Q_h. \tag{28b}$$

The well-posedness of (28) is a standard result, for example, refer to [16], Theorem 15.3.

4.1. Error estimate. We are now ready to state the error estimates. First, the discretization error is bounded by the following result.

Proposition 4.1. *Let $(u^\varepsilon, p^\varepsilon)$ and $(u_h^\varepsilon, p_h^\varepsilon)$ be the solutions of* (22) *and* (28), *respectively. Then we have*

$$\|u^\varepsilon - u_h^\varepsilon\|_{H^1} + \|p^\varepsilon - p_h^\varepsilon\|_{L^2} \leqslant C^{**} h \|\chi^\varepsilon\|_{H^1}, \tag{29a}$$

$$\|u^\varepsilon - u_h^\varepsilon\|_{L^2} \leqslant C^{**} h^2 \|\chi^\varepsilon\|_{H^1}, \tag{29b}$$

where C^{**} denotes a positive constant depending only on Ω, Γ, $\|g\|_{W^{2-1/p,p}}$. Moreover, if χ^ε is given by (24), *then we derive*

$$\|u^\varepsilon - u_h^\varepsilon\|_{H^1} + \|p^\varepsilon - p_h^\varepsilon\|_{L^2} \leqslant C^{**} \frac{h}{\sqrt{\varepsilon}}, \tag{30a}$$

$$\|u^\varepsilon - u_h^\varepsilon\|_{L^2} \leqslant C^{**} \frac{h^2}{\sqrt{\varepsilon}}. \tag{30b}$$

P r o o f. It is well known that the finite element approximation makes the optimal approximation. That is,

$$\|u^\varepsilon - u_h^\varepsilon\|_{H^1} + \|p^\varepsilon - p_h^\varepsilon\|_{L^2} \leqslant C_4 \inf_{(v_h,q_h)\in V_h\times Q_h} \left(\|u^\varepsilon - v_h\|_{H^1} + \|p^\varepsilon - q_h\|_{L^2}\right),$$

where $C_4 > 0$ depends only on Ω. Refer to [16], Theorem 15.3, for example. Applying the standard interpolation error estimates and the stability result (14), we obtain that

$$\|u^\varepsilon - u_h^\varepsilon\|_{H^1} + \|p^\varepsilon - p_h^\varepsilon\|_{L^2} \leqslant C_5 h \|f^\varepsilon\|_{L^2}.$$

Furthermore, by virtue of the duality technique in [7], Theorem 1.9, §1, Chapter II, we have

$$\|u^\varepsilon - u_h^\varepsilon\|_{L^2} \leqslant C_5 h^2 \|f^\varepsilon\|_{L^2}.$$

Therein, C_5 depends only on Ω. Consequently, estimates (29) are obtained with $C^{**} = C_0 C_5 \|\tilde{g}\|_{W^{2-1/p,p}} \|\tilde{n}\|_{L^\infty}$, since

$$\|f^\varepsilon\|_{L^2} = \|\tilde{g}(\nabla\chi^\varepsilon \cdot \tilde{n})\|_{L^2} \leqslant \|\tilde{g}\|_{L^\infty} \|\tilde{n}\|_{L^\infty} \|\nabla\chi^\varepsilon\|_{L^2}.$$

When χ^ε is given by (24), we continue to calculate as

$$\begin{aligned}\|\nabla\chi^\varepsilon\|_{L^2(\Omega)} &= \Big\|\nabla\frac{\operatorname{dist}(x,\Gamma)}{\varepsilon}\Big\|_{L^2(\Gamma^\varepsilon)} \\ &\leqslant \frac{1}{\varepsilon}\operatorname{meas}(\Gamma^\varepsilon)^{1/2} \|\operatorname{dist}(x,\Gamma)\|_{W^{1,\infty}} = \frac{1}{\sqrt{\varepsilon}} \|\operatorname{dist}(x,\Gamma)\|_{W^{1,\infty}}.\end{aligned}$$

□

At this stage, we apply Propositions 3.2 and 4.1 to deduce the total error estimate which is the main theorem in this paper.

Theorem 4.1. *Let (u,p) and $(u_h^\varepsilon, p_h^\varepsilon)$ be, respectively, the solutions to* (20) *and* (28) *with* (24). *Then we have*

$$\|u - u_h^\varepsilon\|_{H^1} + \|p - p_h^\varepsilon\|_{L^2} \leqslant C\Big(\sqrt{\varepsilon} + \frac{h}{\sqrt{\varepsilon}}\Big), \tag{31a}$$

$$\|u - u_h^\varepsilon\|_{L^2} \leqslant C\Big(\sqrt{\varepsilon} + \frac{h^2}{\sqrt{\varepsilon}}\Big), \tag{31b}$$

where C denotes a positive constant depending only on Ω, Γ, and $\|g\|_{W^{2-1/p,p}}$. In particular, if $\varepsilon = c_1 h$ with a positive constant c_1, then

$$\|u - u_h^\varepsilon\|_{H^1} + \|p - p_h^\varepsilon\|_{L^2} \leqslant C\sqrt{h}. \tag{32}$$

Else if $\varepsilon = c_1 h^2$, *then*

$$\|u - u_h^\varepsilon\|_{L^2} \leqslant Ch, \tag{33}$$

where C *denotes a positive constant depending only on* Ω, Γ, $\|g\|_{W^{2-1/p,p}}$, *and* c_1.

R e m a r k 4.2. Numerical approximations of other singular source terms $\delta(\Gamma, g, x)$ defined by

$$\int_{\mathbb{R}^d} \delta(\Gamma, g, x) f(x)\,\mathrm{d}x = \int_\Gamma g(\theta) f(X(\theta))\,\mathrm{d}\theta, \quad f \in C^q(\mathbb{R}^d) \text{ with some } q, \tag{34}$$

are studied in [20]. Introducing a regularization $\delta^\varepsilon(\Gamma, g, x)$ and a uniform Eulerian grid, the authors consider the quadrature error

$$E = \left| h^d \sum_{j \in \mathbb{Z}^d} \delta^\varepsilon(\Gamma, g, x_j) f(x_j) - \int_\Gamma g(\theta) f(X(\theta))\,\mathrm{d}\theta \right|$$

and report in §3.2 that $E = \mathcal{O}(1)$ when $\delta^\varepsilon(\Gamma, g, x) = \tilde{g}(x)\delta^\varepsilon(\mathrm{dist}(x, \Gamma))$ with $\varepsilon = h, 1.5h$, or $2h$. Here $\delta^\varepsilon(x)$ represents a suitable approximation to the Dirac delta function and $x_j = jh$. On the other hand, our approach corresponds to the case $\delta(\Gamma, g, x) = \tilde{g}\nabla\chi \cdot \tilde{n}$, where $\nabla\chi \cdot \tilde{n}$ is approximated by the function of $\mathrm{dist}(x, \Gamma)$ in (24). As in Theorem 4.1, when we use the derivative of characteristic function instead of the Dirac delta, we can obtain the error of order $\mathcal{O}(h^{1/2})$ in the $H^1 \times L^2$ norm for $\varepsilon = c_1 h$.

5. Numerical examples

In this section, we show some results of numerical experiments to verify our theoretical results. We consider the Stokes interface problem

$$-\nu\Delta u_i + \nabla p_i = 0, \quad \nabla \cdot u_i = 0 \quad \text{in } \Omega_i,\ i = 0, 1, \tag{35a}$$

$$u_i = 0 \quad \text{on } \partial\Omega_i \setminus \Gamma, \tag{35b}$$

$$u_0 = u_1, \quad \tau_0 + \tau_1 = g \quad \text{on } \Gamma, \tag{35c}$$

for $\nu > 0$.

We want to obtain the solution to (35) numerically. To do this, for f^ε given by (21), we consider the stationary Stokes problem

$$-\nu\Delta u + \nabla p = f \quad \text{in } \Omega, \quad \nabla \cdot u = 0 \quad \text{in } \Omega, \quad u = 0 \quad \text{on } \partial\Omega, \tag{36}$$

and its regularized version

$$-\nu\Delta u^\varepsilon + \nabla p^\varepsilon = f^\varepsilon \text{ in } \Omega, \quad \nabla\cdot u^\varepsilon = 0 \quad \text{in } \Omega, \quad u^\varepsilon = 0 \quad \text{on } \partial\Omega. \tag{37}$$

Then, we solve the following finite element approximation

$$a(u_h^\varepsilon, v_h) + b(p_h^\varepsilon, v_h) = (f^\varepsilon + \iota, v_h)_{L^2} \quad \forall\, v_h \in V_h, \tag{38a}$$

$$b(q_h, u_h^\varepsilon) = 0 \quad \forall\, q_h \in Q_h. \tag{38b}$$

The first example corresponds to the case $\partial\Omega \cap \overline{\Gamma} = \emptyset$. We refer to [3], §7.1 to provide an analytical solution. Setting $\Omega = (0,1)^2 \subset \mathbb{R}^2$ and $\Gamma = \{(x,y) \in \Omega;$ $\sqrt{(x-0.5)^2 + (y-0.5)^2} = R\}$ for $R > 0$, we impose $\nu = 1$, $g = n/R$ and $\iota = (0,0)$. Functions $g, n \in C^\infty(\Gamma)^2$ have canonical extensions to $C^\infty(\Omega \setminus \{0\})^2$. Indeed, we have $\tilde{g}, \tilde{n} \in W^{1,\infty}(\Omega)^2$. Then the problem (35) (or equivalently the problem (36)) has the exact solution

$$u = 0, \quad p(x) = \begin{cases} \dfrac{1}{R} - \pi R, & |x - c_0| \leqslant R, \\ -\pi R, & |x - c_0| > R, \end{cases} \tag{39}$$

where $c_0 = (1/2, 1/2)$. Below, let $R = 1/4$.

For regularization, we simply use χ^ε as described in (24). For discretization, we employ the uniform triangulation over $\overline{\Omega}$, which is divided into N^2 isosceles right triangles with $h = \sqrt{2}/N$. Hence, it is ensured by Theorem 4.1 that

- ▷ if $\varepsilon = c_1 h$ then $\|u - u_h^\varepsilon\|_{H^1} + \|p - p_h^\varepsilon\|_{L^2} \leqslant C\sqrt{h}$,
- ▷ if $\varepsilon = c_1 h^2$ then $\|u - u_h^\varepsilon\|_{L^2} \leqslant Ch$.

In the numerical experiments, we only deal with the case $\varepsilon = c_1 h$, because it is not possible to implement the case $\varepsilon = c_1 h^2$. The parameter ε represents the width of the band around the interface in which the characteristic function is smoothed. If this width is much smaller than the mesh size h, then we fail to capture the values of $\nabla\chi^\varepsilon$ in computation. To verify the result of Theorem 4.1, we compute the following quantities:

$$E_h^{(1)} = \|u - u_h^\varepsilon\|_{L^2}, \quad E_h^{(2)} = \|u - u_h^\varepsilon\|_{H^1}, \quad E_h^{(3)} = \|p - p_h^\varepsilon\|_{L^2},$$

and

$$\varrho_h^{(j)} = \frac{\log E_{2h}^{(j)} - \log E_h^{(j)}}{\log(2h) - \log h}, \quad j = 1, 2, 3.$$

Herein, ε is chosen as $\varepsilon = h$. All computations were done using `FreeFEM++` [8]. The result is reported in Table 1. We can infer that the convergence rate of the $H^1 \times L^2$

error of (u, p) is 0.5 and the L^2 error of u is of order 1, which supports our theoretical results. We also observe that the L^2 error of u does not converge when $h = 0.00883$. This is possibly due to numerical oscillations around Γ shown in Figure 2. Numerical oscillations and non-convergence were observed also for other values of c_1.

h	$E_h^{(1)}$	$\varrho_h^{(1)}$	$E_h^{(2)}$	$\varrho_h^{(2)}$	$E_h^{(3)}$	$\varrho_h^{(3)}$
0.14142	8.624e−06	—	1.645e−02	—	9.6066	—
0.07071	1.297e−06	1.366	5.420e−03	0.800	5.414e−01	2.074
0.03535	4.597e−07	0.748	3.045e−03	0.415	2.914e−01	0.446
0.01767	1.193e−07	0.972	1.523e−03	0.499	1.458e−01	0.499
0.00883	6.068e−07	−1.172	9.656e−04	0.328	7.448e−02	0.484

Table 1. Convergence rates of Example 1 for $\varepsilon = h$.

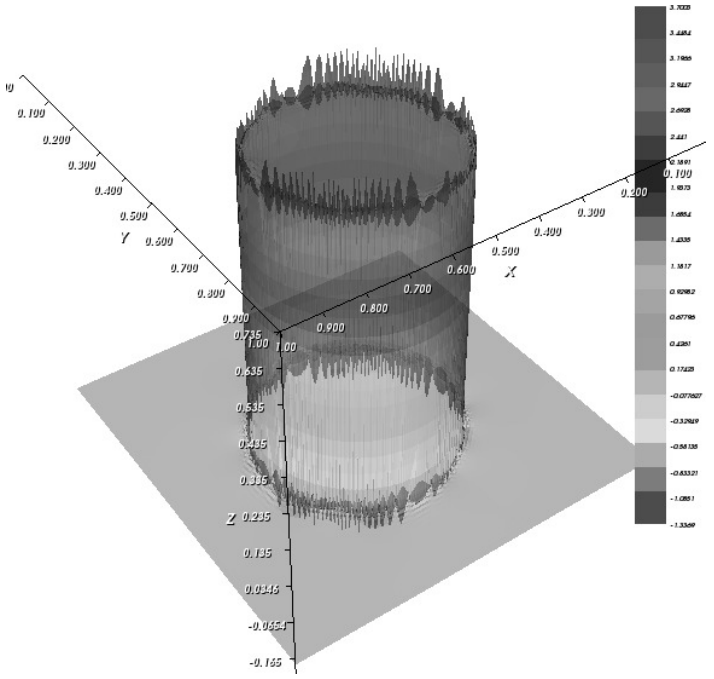

Figure 2. Pressure p_h^ε of Example 1 for $h = 0.00883$. The pressure becomes a discontinuous function across the interface Γ where numerical oscillations are observed.

For further investigation, we employ the arctangential approximation (27) for χ^ε instead of (24). In this case, the function χ^ε becomes smooth in $\Omega \setminus \{0\}$. The results of computation of the same quantities are reported in Table 2 and Figure 3. We observe no numerical oscillations in Figure 3 and that the L^2 error of u is rather

of order 1.5. This implies that our L^2 estimate (33) can be probably improved. However, numerical oscillations reappeared when ε was taken as h^2.

h	$E_h^{(1)}$	$\varrho_h^{(1)}$	$E_h^{(2)}$	$\varrho_h^{(2)}$	$E_h^{(3)}$	$\varrho_h^{(3)}$
0.14142	3.063e−08	—	1.376e−04	—	5.2155	—
0.07071	3.843e−09	1.497	5.403e−05	0.674	6.245e−01	1.530
0.03535	4.472e−10	1.551	2.440e−05	0.573	3.472e−01	0.423
0.01767	5.431e−11	1.520	1.185e−05	0.521	1.842e−01	0.457
0.00883	6.713e−12	1.508	5.869e−06	0.506	9.498e−02	0.477

Table 2. Convergence rates of Example 1 for (27) with $\varepsilon = h$.

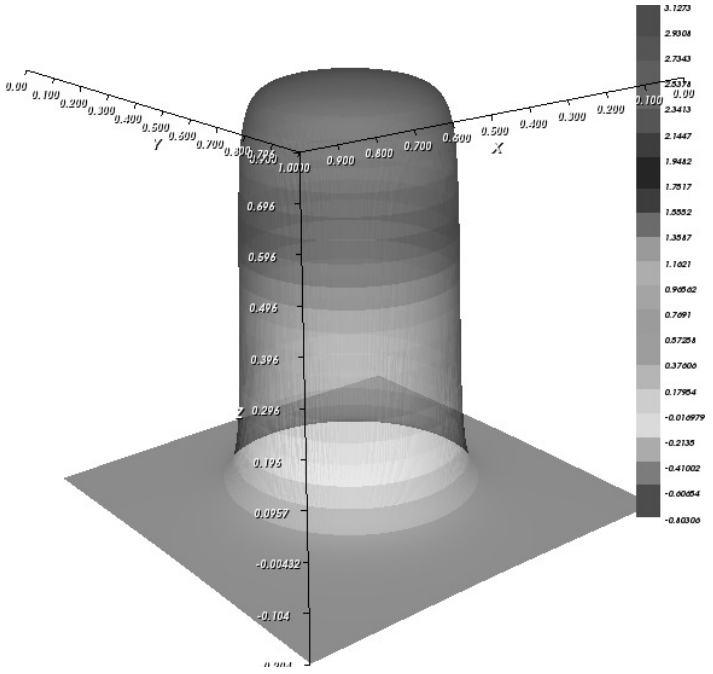

Figure 3. Pressure p_h^ε of Example 1 using (27) for $h = 0.00883$.

The second example corresponds to the case $\partial\Omega \cap \overline{\Gamma} \neq \emptyset$. We set $\Omega = (-1,1) \times (0,1) \subset \mathbb{R}^2$ and Γ lying on the y axis. In this case, we have the exact solution

$$u = 0 \quad \text{and} \quad p = \begin{cases} -\frac{1}{2} & (x > 0), \\ \frac{1}{2} & (x \leqslant 0) \end{cases} \quad \text{in } \Omega$$

to (35) for $g = n = (-1, 0)$. We compute the same quantities as in Example 1 and report them in Tables 3–4 for χ^ε given by (24) and in Table 5 for the arctangential approximation (27). Figure 4 shows the pressure p_h^ε for (24) with $\varepsilon = h$ and $\varepsilon = 2h$.

h	$E_h^{(1)}$	$\varrho_h^{(1)}$	$E_h^{(2)}$	$\varrho_h^{(2)}$	$E_h^{(3)}$	$\varrho_h^{(3)}$
0.14142	1.601e−04	—	8.266e−03	—	6.889e−02	—
0.07071	5.941e−05	1.430	5.983e−03	0.466	4.851e−02	0.506
0.03535	2.149e−05	1.467	4.279e−03	0.483	3.708e−02	0.387
0.01767	7.682e−06	1.484	3.042e−03	0.491	3.067e−02	0.273
0.00883	2.731e−06	1.492	2.157e−03	0.496	2.715e−02	0.175

Table 3. Convergence rates of Example 2 for (24) with $\varepsilon = h$.

h	$E_h^{(1)}$	$\varrho_h^{(1)}$	$E_h^{(2)}$	$\varrho_h^{(2)}$	$E_h^{(3)}$	$\varrho_h^{(3)}$
0.14142	4.689e−05	—	2.329e−03	—	1.901e−01	—
0.07071	1.758e−05	1.415	1.696e−03	0.457	1.370e−01	0.472
0.03535	6.386e−06	1.460	1.216e−03	0.479	9.785e−02	0.485
0.01767	2.287e−06	1.481	8.661e−04	0.490	6.960e−02	0.491
0.00883	8.139e−07	1.490	6.145e−04	0.495	4.945e−02	0.492

Table 4. Convergence rates of Example 2 for (24) with $\varepsilon = 2h$.

h	$E_h^{(1)}$	$\varrho_h^{(1)}$	$E_h^{(2)}$	$\varrho_h^{(2)}$	$E_h^{(3)}$	$\varrho_h^{(3)}$
0.14142	1.364e−05	—	8.511e−04	—	2.208e−01	—
0.07071	4.906e−06	1.475	6.082e−04	0.484	1.593e−01	0.470
0.03535	1.749e−06	1.487	4.323e−04	0.492	1.138e−01	0.485
0.01767	6.210e−07	1.494	3.065e−04	0.496	8.086e−02	0.493
0.00883	2.200e−07	1.497	2.170e−04	0.498	5.731e−02	0.496

Table 5. Convergence rates of Example 2 for (27) with $\varepsilon = h$.

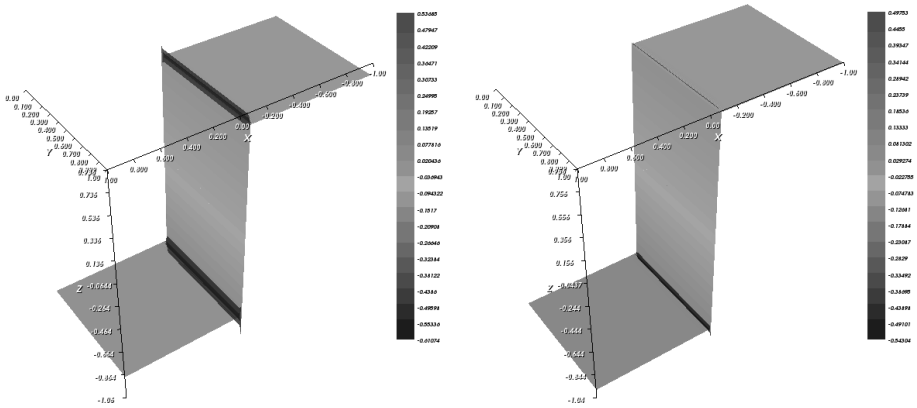

Figure 4. Pressure p_h^ε of Example 2 for (24) with $\varepsilon = h$ (left) and $\varepsilon = 2h$ (right) when $h = 0.00883$.

We observe that in Figure 4 the numerical oscillations decrease as the values of c_1 in $\varepsilon = c_1 h$ increase, while the reduction of convergence rates of the pressure in Table 3 is recovered in Table 4. In Table 5, this loss of convergence rates is not observed. We can infer the same convergence rates as in Example 1, which supports our theoretical results again.

Appendix A. Proof of (15)

In this appendix, we prove the equation

$$\int_\Gamma g \cdot \varphi \,\mathrm{d}\Gamma = \langle \tilde{g}(\nabla\chi \cdot \tilde{n}), \varphi \rangle \quad \forall\, \varphi \in C_0^\infty(\Omega)^d. \tag{15}$$

P r o o f. First, we note that the assumptions (A1) and (A2) imply $\tilde{g} \in W^{1,\infty}(\Omega)^d$ and $\tilde{n} \in H^1(\Omega)^d$. Then we have $\tilde{g}(\nabla\chi \cdot \tilde{n}) \in H^{-1}(\Omega)^d$ by the representation

$$\tilde{g}(\nabla\chi \cdot \tilde{n}) = \sum_{i=0}^{d} \frac{\partial}{\partial x_i}(\tilde{g}\chi\tilde{n}_i) - \sum_{i=0}^{d} \chi \frac{\partial}{\partial x_i}(\tilde{g}\tilde{n}_i).$$

Furthermore, for all $\varphi \in C_0^\infty(\Omega)^d$, the function $(\tilde{g} \cdot \varphi)\tilde{n}$ belongs to $H_0^1(\Omega)^d$. Thus, we have

$$\begin{aligned}\langle \tilde{g}(\nabla\chi \cdot \tilde{n}), \varphi \rangle &= \langle \nabla\chi, (\tilde{g} \cdot \varphi)\tilde{n} \rangle = -\langle \chi, \operatorname{div}((\tilde{g} \cdot \varphi)\tilde{n}) \rangle \\ &= -\int_{\Omega_0} \operatorname{div}((\tilde{g} \cdot \varphi)\tilde{n}) \,\mathrm{d}x = -\int_\Gamma (g \cdot \varphi) n_1 \cdot (-n_1) \,\mathrm{d}\Gamma.\end{aligned}$$

□

A c k n o w l e d g e m e n t. I would like to thank professor Norikazu Saito for bringing this topic to my attention and encouraging me through valuable discussions. I also thank the anonymous referees for insightful comments and suggestions.

References

[1] *R. A. Adams, J. J. F. Fournier*: Sobolev Spaces. Pure and Applied Mathematics 140, Academic Press, New York, 2003.
[2] *D. Boffi, L. Gastaldi, L. Heltai*: Numerical stability of the finite element immersed boundary method. Math. Models Methods Appl. Sci. *17* (2007), 1479–1505.
[3] *D. Boffi, L. Gastaldi, L. Heltai, C. S. Peskin*: On the hyper-elastic formulation of the immersed boundary method. Comput. Methods Appl. Mech. Eng. *197* (2008), 2210–2231.
[4] *M. Dauge*: Stationary Stokes and Navier-Stokes systems on two- or three-dimensional domains with corners. I: Linearized equations. SIAM J. Math. Anal. *20* (1989), 74–97.

[5] *J. M. Floryan, H. Rasmussen*: Numerical methods for viscous flows with moving boundaries. Appl. Mech. Rev. *42* (1989), 323–341.
[6] *H. Fujita, H. Kawahara, H. Kawarada*: Distribution theoretic approach to fictitious domain method for Neumann problems. East-West J. Numer. Math. *3* (1995), 111–126.
[7] *V. Girault, P.-A. Raviart*: Finite Element Methods for Navier-Stokes Equations. Theory and Algorithms. Springer Series in Computational Mathematics 5, Springer, Berlin, 1986.
[8] *F. Hecht*: New development in freefem++. J. Numer. Math. *20* (2012), 251–265.
[9] *T. Y. Hou*: Numerical solutions to free boundary problems. Acta Numerica 1995 (A. Iserles, ed.). Cambridge University Press, Cambridge, 1995, pp. 335–415.
[10] *R. B. Kellogg, J. E. Osborn*: A regularity result for the Stokes problem in a convex polygon. J. Funct. Anal. *21* (1976), 397–431.
[11] *J. Nečas*: Direct Methods in the Theory of Elliptic Equations. Springer Monographs in Mathematics, Springer, Berlin, 2012.
[12] *K. Ohmori, N. Saito*: On the convergence of finite element solutions to the interface problem for the Stokes system. J. Comput. Appl. Math. *198* (2007), 116–128.
[13] *C. S. Peskin*: Flow patterns around heart valves: a numerical method. J. Comput. Phys. *10* (1972), 252–271.
[14] *C. S. Peskin*: Numerical analysis of blood flow in the heart. J. Comput. Phys. *25* (1977), 220–252.
[15] *C. S. Peskin*: The immersed boundary method. Acta Numerica *11* (2002), 479–517.
[16] *A. Quarteroni*: Numerical Models for Differential Problems. MS&A. Modeling, Simulation and Applications 8, Springer, Milano, 2014.
[17] *N. Saito, Y. Sugitani*: Convergence of the immersed-boundary finite-element method for the Stokes problem. ArXiv:1611.07172.
[18] *R. Scardovelli, S. Zaleski*: Direct numerical simulation of free-surface and interfacial flow. Annual Review of Fluid Mechanics. Annu. Rev. Fluid Mech. 31, Annual Reviews, Palo Alto, 1999, pp. 567–603.
[19] *M. Tabata*: Finite element schemes based on energy-stable approximation for two-fluid flow problems with surface tension. Hokkaido Math. J. *36* (2007), 875–890.
[20] *A.-K. Tornberg, B. Engquist*: Numerical approximations of singular source terms in differential equations. J. Comput. Phys. *200* (2004), 462–488.

Author's address: *Yoshiki Sugitani*, WPI-Advanced Institute for Materials Research (WPI-AIMR), Tohoku University, 2-1-1 Katahira, Aoba-ku, Sendai, Miyagi, Japan 980-8577, e-mail: `yoshiki.sugitani@tohoku.ac.jp`.